INSTITUTE OF FLUID-FLOW MACHINERY
POLISH ACADEMY OF SCIENCES

TRANSACTIONS OF THE INSTITUTE OF FLUID-FLOW MACHINERY

112

WYDAWNICTWO IMP PAN

GDAŃSK 2003

EDITORIAL AND PUBLISHING OFFICE

IFFM Publishers (Wydawnictwo IMP), Institute of Fluid Flow Machinery, Fiszera 14, 80-952 Gdańsk, Poland, Tel.: +48(58)3411271 ext. 141, Fax: +48(58)3416144, E-mail: esli@imp.gda.pl

Financial support of publication of this journal is provided by the State Committee for Scientific Research, Warsaw, Poland

Terms of subscription

Subscription order and payment should be directly sent to the Publishing Office

Warunki prenumeraty w Polsce

Wydawnictwo ukazuje się przeciętnie dwa lub trzy razy w roku. Cena numeru wynosi 20,- zł + 5,- zł koszty wysyłki. Zamówienia z określeniem okresu prenumeraty, nazwiskiem i adresem odbiorcy należy kierować bezpośrednio do Wydawcy (Wydawnictwo IMP, Instytut Maszyn Przepływowych PAN, ul. Gen. Fiszera 14, 80-952 Gdańsk). Osiągalne są również wydania poprzednie. Prenumerata jest również realizowana przez jednostki kolportażowe RUCH S.A. właściwe dla miejsca zamieszkania lub siedziby prenumeratora. W takim przypadku dostawa następuje w uzgodniony sposób.

ISSN 0079-3205

TRANSACTIONS OF THE INSTITUTE OF FLUID-FLOW MACHINERY
Appears since 1960

Aims and Scope

Transactions of the Institute of Fluid-Flow Machinery have primarily been established to publish papers from four disciplines represented at the Institute of Fluid-Flow Machinery of Polish Academy of Sciences, such as:

- Liquid flows in hydraulic machinery including exploitation problems,
- Gas and liquid flows with heat transport, particularly two-phase flows,
- Various aspects of development of plasma and laser engineering,
- Solid mechanics, machine mechanics including exploitation problems.

The periodical, where originally were published papers describing the research conducted at the Institute, has now appeared to be the place for publication of works by authors both from Poland and abroad. A traditional scope of topics has been preserved.

Only original and written in English works are published, which represent both theoretical and applied sciences. All papers are reviewed by two independent referees.

TRANSACTIONS OF THE INSTITUTE OF FLUID-FLOW MACHINERY

No. 112, 2003, 57-74

YUMING CHEN*, MANFRED GROLL, RAINER MERTZ and RUDI KULENOVIC

Force analysis for isolated bubbles growing from smooth and evaporator tubes

Institute of Nuclear Technology and Energy Systems (IKE), University of Stuttgart, Pfaffenwaldring 31, 70569 Stuttgart, Germany

Abstract

Various forces acting on a bubble growing on a horizontal smooth and enhanced tube have been evaluated by using the measured geometric bubble data. Great effort has been made to accurately evaluate the dynamic forces. It has been shown that the dynamic forces play a more important role in the bubble growth on an enhanced surface than on a smooth surface. A correlation for predicting the bubble departure diameter from an enhanced tube has been derived from the force balance. This correlation has a form similar to that commonly used for smooth tubes while baring a different physical meaning.

Keywords: Force; Bubble dynamics; Pool boiling; Enhanced tube

Nomenclature

C, C_0, C_1	–	coefficients, –	H	–	bubble height, m
C_d	–	drag coefficient, –	p	–	pressure, Pa
D	–	bubble diameter, m	R	–	bubble radius, m
D_C	–	contact diameter, m	R_t	–	radius shown in Fig. 3, m
D_d	–	departure diameter, m	S	–	height of bubble mass center, m
F_B	–	buoyancy force, N	t	–	time, s
F_{BI}	–	bubble inertia force, N	u	–	bubble front velocity, m/s
F_{CP}	–	contact pressure force, N	u_0	–	velocity of mass center
F_D	–	drag force, N	U	–	bubble rise velocity, m/s
F_{LI}	–	liquid inertia force, N	V	–	bubble volume, m^3
F_{ST}	–	surface tension force, N	V_C	–	shaded volume shown in Fig. 3, m^3
g	–	acceleration of gravity, m/s^2	V_L	–	volume of virtual added mass, m^3

*Corresponding author. E-mail address: chen@ike.uni-stuttgart.de

μ – dynamic viscosity, kg/ms
θ – contact angle, deg
ρ – density, kg/m^3
σ – surface tension

Subscripts

L – liquid phase
V – vapour phase

1 Introduction

Enhanced structured surfaces become more widely used in industries due to their excellent boiling heat transfer performances. Although there is a large number of investigations concerning the bubble dynamics on smooth surfaces, studies of bubble dynamics on enhanced structured surfaces are very limited. In order to better understand the mechanisms of enhanced boiling, a detailed comparison of bubble dynamics between smooth and enhanced tubes has been made [1]. The present work aims at revealing the forces acting on a growing bubble from smooth and enhanced tubes.

Force analysis has been performed for a growing bubble by a number of investigators with the main purpose of predicting the bubble departure diameter [2-14]. Without exception, all these works deal with a bubble growing on a plain heated surface. Due to the lack of geometric bubble data, only a few works presented the calculated results of various forces acting on a growing bubble throughout the bubble lifetime [4,5,7,14]. Some of these results show a large positive net force far before the detachment point, which is obviously unreasonable and is thought to be due to the inaccurate evaluation of the dynamic forces (inertia and drag). Thus the accurate evaluation of various forces acting on a growing bubble is the main aim of this work.

2 Experimental set-up and investigated tubes

Pool boiling experiments were carried out with a smooth tube and an enhanced tube. Both tubes are made of carbon steel St35.8, have a diameter of 19 mm and a length of 115 mm. The surface roughness for the smooth tube is $R_a = 1.1$ μm. The enhanced tube consists of sub-surface tunnels and surface pores (Fig. 1). The pores show an elliptic shape and are not uniform in size. Typically, the average width of an elliptic pore is 0.062 mm and the length is about 0.4 mm. The equivalent pore diameter is about 0.16 mm.

Figure 2 shows a scheme of the experimental set-up. The pressure vessel (maximum pressure 16 bar) with the test tube is connected to two cryostats for

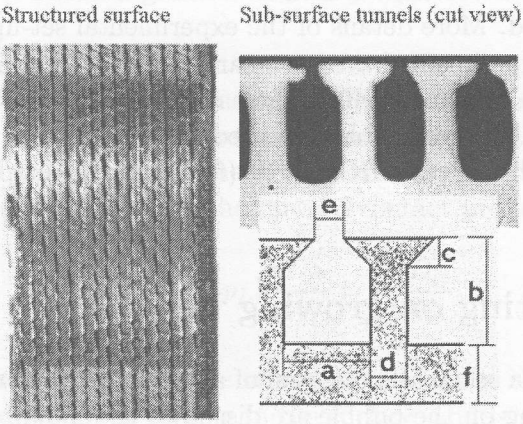

Figure 1. Surface and sub-surface tunnels of enhanced tube.

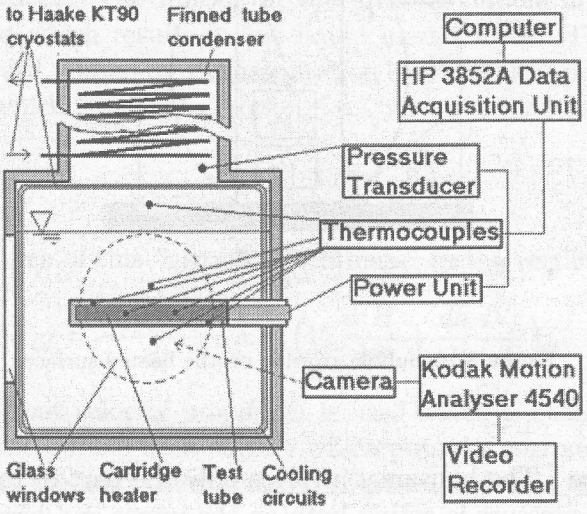

Figure 2. Scheme of experimental set-up.

controlling the temperature of the liquid as well as the vapour. For the smooth tube propane and iso-butane are used as working fluids. For the enhanced tube only propane is used. More details of the experimental set-up are given in [1].

Visualisation experiments have been carried out with a high speed video system (Kodak Motion Analyser 4540, highest recording rate: 40500 frames/s). Cold light sources with fiber optic cables are used for illumination. The digital images were processed by the software IKE_DBV (for details see http://www-ew.ike.uni-stuttgart.de).

3 Forces acting on growing bubbles

Figure 3 shows a schematic diagram of a bubble growing on a heated surface. Various forces acting on the bubble are discussed as follows.

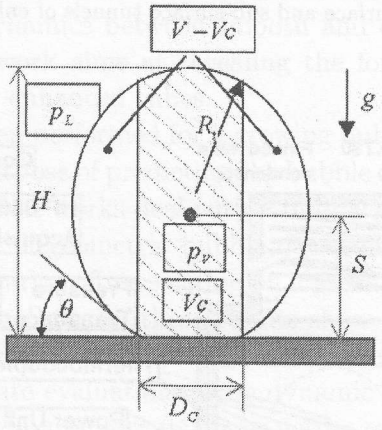

Figure 3. A bubble growing on the heated surface.

Buoyancy force The buoyancy involves only the part of the bubble $V - V_C$ for which liquid pressure is acting both on the upper and lower portions of the liquid-vapour interface [5,7].

$$F_B = (V - V_C)\rho_L g - V\rho_V g \,. \tag{1}$$

Here, V_C is the shaded volume shown in Fig. 3 which is approximately given by

$$V_C = \frac{\pi D_C^2}{4} H \,. \tag{2}$$

The use of this partial volume is based on the assumption that there is a dry area at the bubble base. This has been proved by a number of investigations [15-17].

Contact pressure force The contact pressure force was first used by Cochran et al. [5] to account for the pressure forces on the shaded volume shown in Fig. 3. Assuming the top of the shaded volume to be spherical with radius R_t, and p_L, p_V not to vary over this area, provides the upward contact pressure force

$$F_{CP} = (p_V - p_L)\frac{\pi D_C^2}{4} = \frac{\pi\sigma D_C^2}{2R_t} . \tag{3}$$

Surface tension force The surface tension force acts at the circumference of the contact area and holds the bubble to the surface, and is given by

$$F_{ST} = \pi D_C \sigma \sin\theta . \tag{4}$$

In [10,11], $\theta = \pi/2$ was assumed at the instance of bubble departure.

Liquid inertia force The motion of the growing bubble interacts with the surrounding liquid which results in the liquid inertia force. This force can be upward or downward. Based on the assumption of frictionless potential flow, the volume of liquid which is put into motion, i.e. "virtual added mass", is given by [18] as

$$V_L = \frac{1}{2}\Big(1 + \frac{3}{8}\frac{R^3}{S^3}\Big)V . \tag{5}$$

Thus the inertia force of this "virtual added mass" in the vertical direction is

$$F_{LI} = \frac{d(\rho_L V_L u)}{dt} = \rho_L\Big(V_L\frac{d^2H}{dt^2} + \frac{dh}{dt}\frac{dV_L}{dt}\Big) . \tag{6}$$

Here, the bubble front velocity $u = dh/dt$ is used which is based on the consideration that it is the bubble front surface which puts the surrounding liquid into motion, resulting in the liquid inertia force in vertical direction. When a spherical bubble is assumed, the bubble front velocity can be expressed as $u = 2dR/dt$, as in [8,9,11,19]. In some references (e.g. [4,12,14]), the velocity of the bubble mass center was used in Eq. (6), i.e. $u = dR/dt$. In practice, the bubbles have generally shapes of truncated spheres or truncated ellipsoids. In this case, the use of the bubble height H to calculate the bubble front velocity in Eq. (6) is more appropriate.

Besides the bubble velocity, the accuracy of Eq. (6) is also dependent on how far the real situation comes close to the theoretical expression of Eq. (5). Various

liquid volumes ranging from $V_L = 0.5V$ to $1.0V$ were used in the literature, as listed in Tab. 1. In fact, the former value is the lower limit when $S \gg R$ which happens when the bubble is dramatically elongated, e.g. the bubble grows on an enhanced tube in the later growing stage (Fig. 4), while the latter value is not a theoretical upper limit.

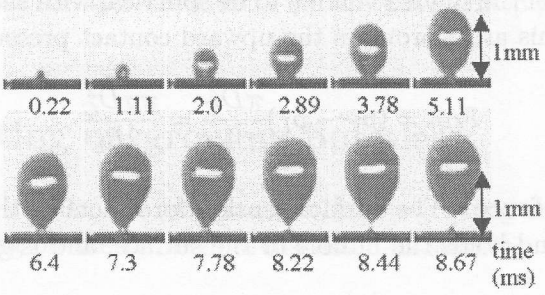

Figure 4. Bubble growing on an enhanced tube (propane, $p = 8.4$ bar, $q = 6.5$ kW/m^2).

Bubble inertia force The bubble inertia force is calculated as

$$F_{BI} = \frac{d(\rho_V V u_0)}{dt} = -\frac{4\pi}{3}\rho_V \left(R^3 \frac{d^2 S}{dt^2} + 3R^2 \frac{dR}{dt}\frac{dS}{dt}\right) \tag{7}$$

here, $u_0 = dS/dt$, is the velocity of bubble mass center.

Drag force The drag force for a moving body (viz. the bubble) is given by

$$F_D = C_d \rho_L \frac{\pi D^2}{4}\frac{U^2}{2} \,. \tag{8}$$

Here, C_d is the drag coefficient and U is the rise velocity of the body. When applying Stokes' law to a rising bubble in a liquid, the drag coefficient C_d can be expressed as [20]

$$C_d = 24\mathrm{Re}^{-1} = \frac{24\mu_L}{\rho_L D U} \,. \tag{9}$$

Equation (9) holds under the assumption of a spherical rigid particle. For a vapour bubble, this means the bubble size should be small enough so as to keep the bubble from deforming. Inserting Eq. (9) into Eq. (8), one obtains

$$F_D = 6\pi R \mu_L U = -6\pi R \mu_L (C\frac{dr}{dt}) \,. \tag{10}$$

Here, C is a coefficient to relate the bubble rise velocity with dR/dt. Different values of are used in the literature, e.g., $C = 1$ in [7], $C \approx 2$ in [4,5], $C = 10/3$ in [10]. For a bubble attached to the wall, the rise velocity which is used to calculate the vertical drag is best represented by the bubble front velocity, thus Eq. (10) changes to

$$F_D = 6\pi R \mu_L \frac{dH}{dt} . \tag{11}$$

For relative big bubbles for which Stokes' law does not hold, an empirical correlation for the drag coefficient is used instead of Eq. (9). In case of boiling of pure propane on an enhanced tube, the drag coefficient is given as (refer [1]),

$$C_d = 0.73 \frac{gD^2 \rho_L}{\sigma} . \tag{12}$$

4 Experimental and calculation results

In order to calculate the aforementioned forces acting on a growing bubble, the time-dependent radius, height of mass center, bubble height, contact diameter D_C and contact angle θ were measured. The radius R is the volume equivalent radius and the radius R_t in Eq. (3) is assumed to be equal to R. It was found that the bubble height H is approximately equal to the sum of radius and height of mass center S (Fig. 5), thus $H = R + S$. In order to calculate the bubble velocities and to evaluate the inertia forces, the first and second derivatives of R, S and H are needed. These derivatives are calculated from the equations which are obtained by fitting the experimental curves with 6^{th}power polynomial functions.

4.1 Enhanced tube

A calculation example is shown here for pool boiling from an enhanced tube (Fig. 1) of pure propane at the saturation temperature of 293 K with heat flux of 6.5 kW/m^2. Fig. 4 shows some pictures of a video sequence which was taken at the rate of 4500 frame/s. The detachment happens at about $t = 8.5$ ms.

Figure 5 shows the curves of bubble radius, height of mass center and bubble height. Far before the bubble departure, the height of the mass center surpasses the bubble radius. Therefore, in this case, the time point at which the height of the mass center surpasses the bubble radius, cannot be considered as the departure point as it was proposed for smooth tubes by some investigators (e.g. [26]).

Figure 6 shows the bubble contact angle ($\sin\theta$) and bubble contact diameter (D_C) changing with time. Similar shapes of the fitted curves are also found in

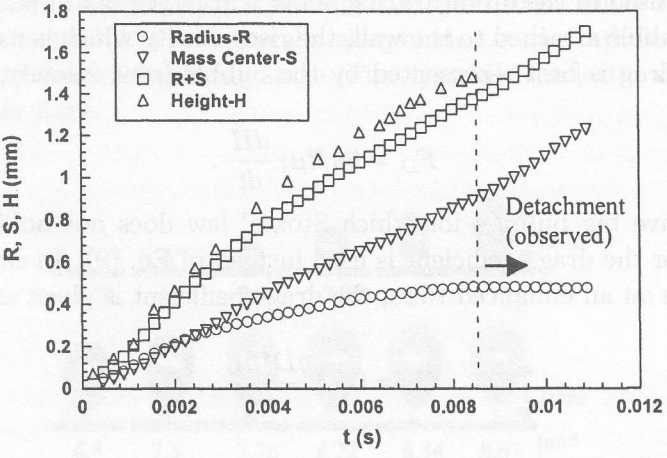

Figure 5. Bubble radius, mass center and bubble height (enchanced tube).

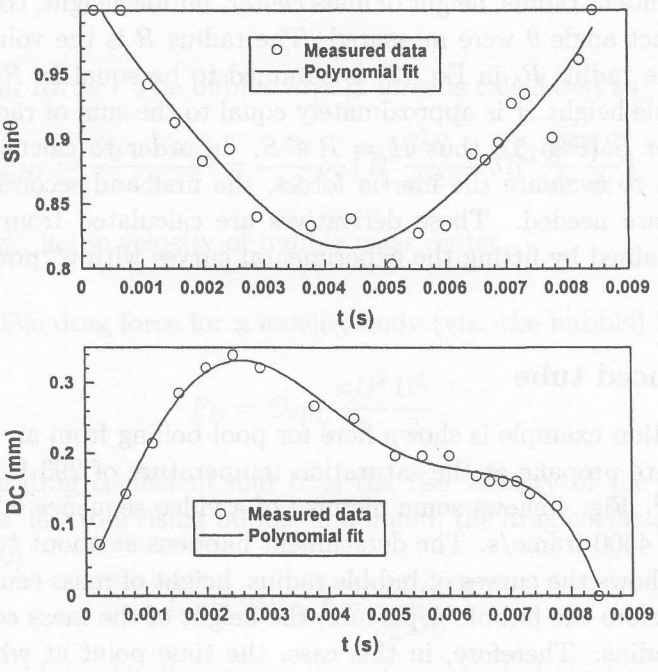

Figure 6. Contact angle ($\sin\theta$) and bubble contact diameter (enhanced tube).

several other measurements. The contact angle goes through a minimum while the contact diameter goes through a maximum. This has also been observed by other investigators for plain surfaces [4,6,15,19]. The difference shown in Fig. 6 is that there is a shoulder on the right-hand-side of the contact diameter curve. The height of the shoulder ranges from 0.15 to 0.2 mm which is very close to the value of the equivalent pore diameter (~0.16 mm).

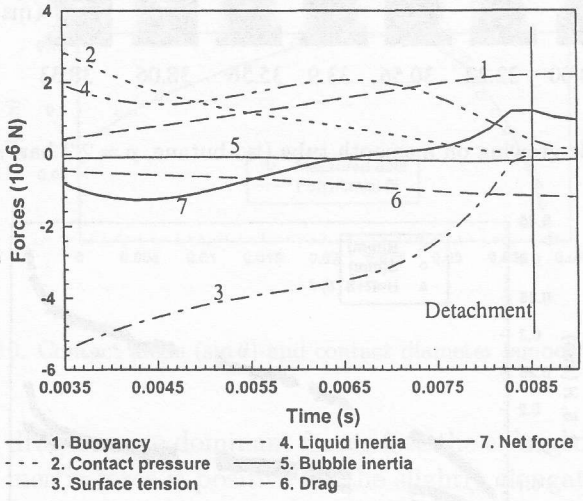

Figure 7. Forces acting on a growing bubble on an enhanced tube.

Figure 7 shows the forces acting on a growing bubble. All forces are important except the bubble inertia force which is only comparable with the other forces at the moment of bubble departure. During most part of the bubble growing period, the liquid inertia force acts upward and pulls the bubble to an elongated shape. The non-zero net force is relatively small compared with results from other investigators [4,7,14]. At the time near bubble detachment, the buoyancy, liquid inertia and drag forces are dominant forces. This indicates the dynamic nature of bubble separation for the enhanced tube.

4.2 Smooth tube

For a smooth tube, a calculation example is shown for pool boiling of isobutane (at saturation temperature of 283 K (2.2 bar), heat flux of 2.0 kW/m^2). Figure 8 shows some pictures of a video sequence which was taken at the rate of 18000 frames/s. Comparing with a bubble growing on an enhanced tube, the bubble growing on a smooth tube is much smaller and looks like a truncated sphere.

Figure 9 shows the curves for bubble growth. Three breaks in these curves are

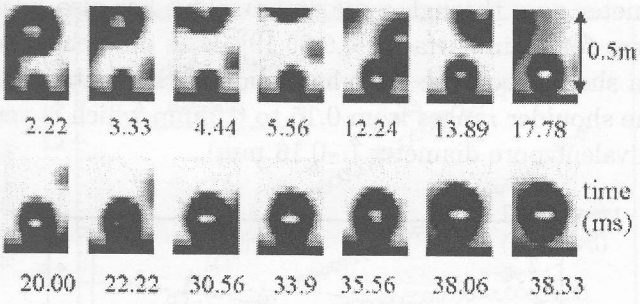

Figure 8. Bubble growing on a smooth tube (iso-butane, $p = 2.2$ bar, $q = 2.0$ kW/m^2.

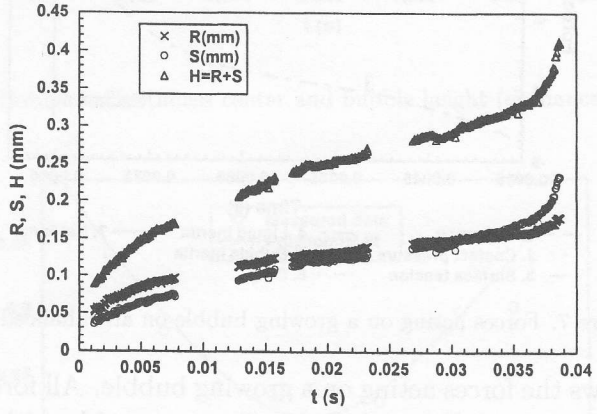

Figure 9. Bubble radius, mass center and bubble height (smooth tube).

due to the temporary contact between the investigated bubble and other bubbles which the software could not discern. Figure 10 shows the time-dependent contact angle ($\sin\theta$) and the contact diameter (D_C). It can be seen from these two figures that during most of the bubble growing period, the bubble equivalent radius is somewhat bigger than the height of the mass center, and the contact diameter is relatively big (about the size of the bubble radius). When the bubble radius surpasses the height of the mass center, the bubble begins to rise, and the contact diameter decreases rapidly.

Figure 11 shows the forces acting on a growing bubble. During most of the bubble lifetime, the contact pressure force and the surface tension force are so large that other forces are negligible. This indicates that dynamic effects are not important for such a small bubble growing on a smooth surface. Only when the bubble begins to detach, these two forces tend to zero quickly, the buoyancy,

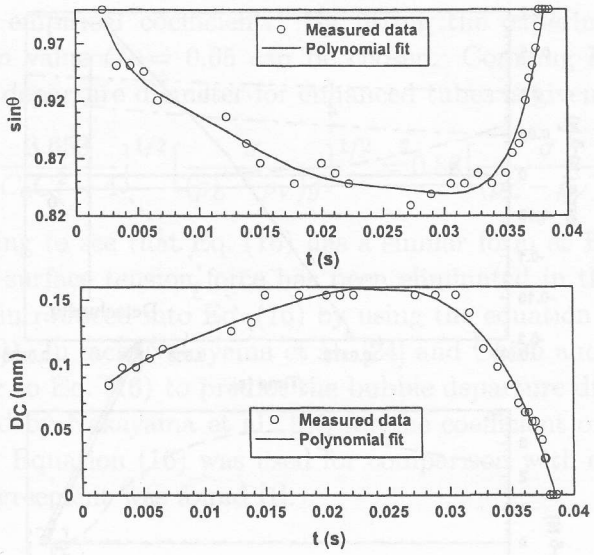

Figure 10. Contact angle ($\sin\theta$) and contact diameter (smooth tube).

liquid inertia and drag become dominant forces (see the enlarged part in Fig. 11). Again, the liquid inertia force is positive for the slightly elongated bubble. From the video sequence (Fig. 8) we see that the bubble detachment happens at about $t = 0.0383$ s.

5 Prediction of bubble departure diameter

For smooth tubes, the surface tension force, though it is reduced to zero very quickly near the detachment point, is a dominant force which holds the bubble to the wall till shortly before detachment (Fig. 11). The buoyancy force, though very small throughout the whole bubble growth period, is the dominant upward force which finally overcomes the downward forces and helps the bubble to detach from the wall. Thus, equating these two forces to predict the bubble departure diameter does not lower the prediction accuracy in practical uses. This leads to a commonly used equation for calculating the departure diameter:

$$D_d = C\Big[\frac{\sigma}{(\rho_L - \rho_V)g}\Big]^{1/3\sim 1/2}, \tag{13}$$

where C is an empirical coefficient depending on fluid and experimental conditions, e.g. pressure. For a perfect spherical bubble the exponent $1/2$ is taken, for a non-spherical bubble this value is between $1/3$ and $1/2$.

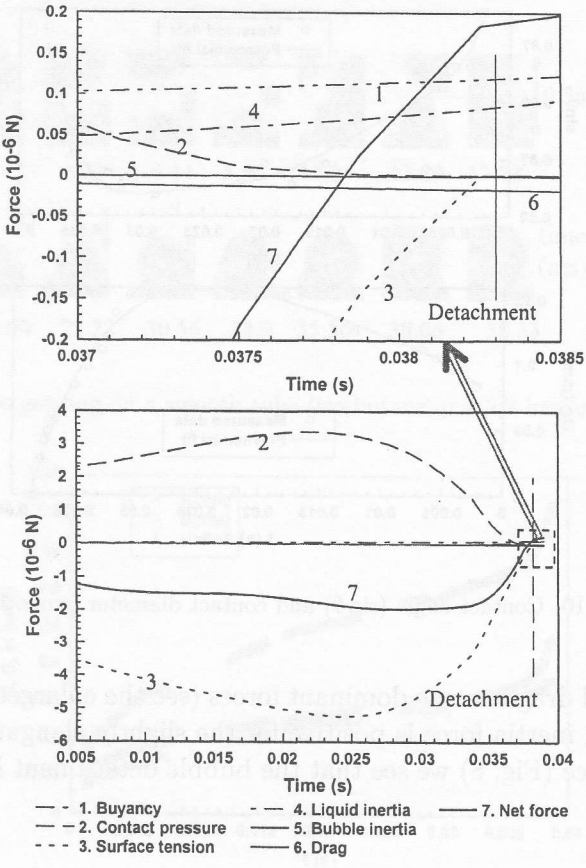

Figure 11. Forces acting on a growing bubble on a smooth tube.

For enhanced tubes, the buoyancy, drag and liquid inertia forces are important. As the bubble comes near detachment, the liquid inertia force decreases quickly while the drag force tends to increase (Fig. 7). If, for simplification, the buoyancy force is assumed to be equal to the drag force multiplied with a coefficient at the detachment point, then

$$\frac{\pi D^3}{6}(\rho_L - \rho_V)g = C_0 C_d \rho_L \frac{\pi D^2}{8} U^2 \,. \tag{14}$$

Equation (12) is used to calculate C_d. C_0 can be calculated from Fig. 7 as $C_0 = 1.823$. U can be represented by the bubble front velocity for a bubble attaching to the wall and is assumed to be proportional to the free bubble rise velocity predicted by wave theory (Mendelson [23]) as

$$U = C_1 \Big(\frac{2\sigma}{D\rho_L} + \frac{gD}{2} \Big)^{1/2} , \tag{15}$$

where C_1 is an empirical coefficient. By fitting the experimental data into Eq. (15), a mean value $C_1 = 0.65$ can be chosen. Combing Eqs. (14,15) and (12), the bubble departure diameter for enhanced tubes is given by

$$D_d = \left[\frac{3.653}{C_0 C_1^2 - 4}\right]^{1/2}\left[\frac{\sigma}{(\rho_L - \rho_V)g}\right]^{1/2} = 0.86\left[\frac{\sigma}{(\rho_L - \rho_V)g}\right]^{1/2}. \quad (16)$$

It is interesting to see that Eq. (16) has a similar form as Eq. (13), though, in this case, the surface tension force has been eliminated in the force balance. However, it is reintroduced into Eq. (16) by using the equation for the terminal velocity (Eq. (15)). In fact, Nakayama et al. [24] and Chien and Webb [25] used equations similar to Eq. (16) to predict the bubble departure diameter. A value of 0.625 was used by Nakayama et al. [24] for the coefficient on the right hand side of Eq. (16). Equation (16) was used for comparison with our experimental data and good agreement was found [1].

6 Discussion

6.1 The accuracy of evaluation of various forces

A video system with a CCD-sensor of 246 × 256 pixel was used in our experiments. The observation area is set to 5 × 5 mm^2 corresponding to a spatial resolution of 0.02 mm/pixel. The uncertainty of the measurement of a one-dimensional image is ±2 pixels. So for a big bubble with 1mm in diameter, the uncertainty of the measurement is ±4%. A much higher uncertainty will result for the measurement of smaller bubbles especially those growing on the smooth tube at the early growing stage.

Besides the experimental technique, the employed methods are even more important for the accurate evaluation of various forces. Many different expressions for evaluating the same force are found in the literature especially for the liquid inertia force (see Section 3). By direct measuring the height of the mass center and the bubble height, the liquid inertia force given by Eq. (6) is thought to give more accurate results. To demonstrate this, Fig. 12 shows the recalculation results of net forces for the enhanced tube by only changing the liquid inertia force term using equations in [4,10,13] instead of Eq. (6). It is clear that much bigger non-zero net forces especially near the detachment point are given by using the other equations than by using Eq. (6). The big negative net force at detachment point is also found in [7] which is partially attributed to the overestimation of the added mass which results in a larger liquid inertia force.

For the calculation of the drag force, the drag coefficient is the most important parameter which takes very different values for small bubbles and for big bubbles. According to bubble sizes, four regions of bubble motion are distinguished. For

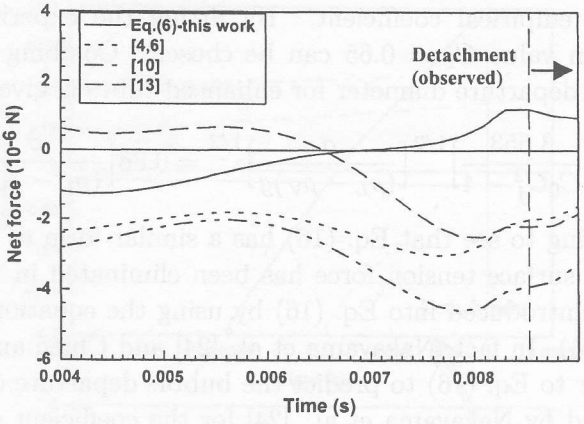

Figure 12. Comparison of calculated net force for enhanced tube by using different equations for liquid inertia force.

each of these regions the correlation for calculating the drag coefficient takes a different form [20]. The correlations we used in this paper (Eqs. (9) and (12)) have been verified by our experimental data [1].

In fact, using methods similar to the present one, the accurate evaluation of various forces acting on a growing bubble on a heating surface involves inherent difficulties both theoretically and experimentally. For example, the expressions for the liquid inertia force are generally based on the assumption of a spherical or hemispherical bubble which is actually an exception, as a result, the determinations of the "virtual added mass", the vapour and liquid velocities are somewhat arbitrary. In [26], the drag is omitted "purposefully" based on the argument that there is actually no wake behind a bubble attached to a wall and therefore no drag. Experimentally, due to the asymmetry of a growing bubble, the numerous bubble geometric parameters are generally given by "representative" values, the real distributions of these parameters are not available and also cannot be applied into the simplified equations. Therefore, the improvement of accuracy using the present method is limited. A completely different method has been developed by the authors for evaluating various forces acting on a growing bubble by simulating the bubble shape [27]. This new method has a clearer theoretical approach and depends less on the measurements and therefore is more accurate than the present one.

6.2 Relative importance of each force during separation stage

Table 1 lists the references which deal with the forces acting on a growing or departing bubble. From this table we can see that, besides buoyancy, the surface

tension and liquid inertia forces are generally considered important during the bubble separation stage, and the bubble inertia is the least important force. Two regimes for bubble separation are generally distinguished, i.e. the quasi-static regime, during which surface tension is considered to be the dominant force, and the dynamic regime during which liquid inertia and/or drag are the dominant forces.

Table 1. References which deal with the forces acting on a growing or departing bubble

Reference	F_B	F_{CP}	F_{ST}	F_{LI} $V_L = CV$	F_{BI}	F_D
[2]	♯		♯			♯
[3]	♯			♯ $C = 11/16$		♯
[4,6]	♯	♯	♯	♯ $C = 11/16$		*
[5,6]	♯	♯	♯	♯ from force balance		*
[7]	♯	♯	♯	♯ $C = 1$		*
[8]	♯		♯	♯ $C = 1$		
[9]	♯	♯	♯	♯ $C = 1/2$	*	♯
[10]	♯		♯	♯ different form		♯
[11]	♯		♯	♯ $C = 1/2$	*	♯
[12]	♯		♯	♯ $C = 1/2$		
[13]	♯			♯ different form		
[14]	♯	♯	♯	* $C = \frac{1}{2}\left(1 + \frac{3}{8}(\frac{R}{S})^3\right)$		*
This work (enhanced)	♯	*	*	♯ $C = \frac{1}{2}\left(1 + \frac{3}{8}(\frac{R}{S})^3\right)$	*	♯
This work (smooth)	♯	*	*	♯ $C = \frac{1}{2}\left(1 + \frac{3}{8}(\frac{R}{S})^3\right)$	*	*

♯ force which was considered important during separation stage;

* force which was considered, but not important during separation stage.

However, it is difficult to determine whether a separation is quasi-static or dynamic. In fact, Cole [2] used the heat flux, Kirichenko [10] used the pressure, Saini et al. [11] used the Jakob number, respectively, as the criterion to distinguish these two regimes. These criteria are generally not clearcut, because in many cases both the static and dynamic forces are equally important (Tab. 1). However, when combining all these forces it would not be possible to derive an analytical correlation for the departure diameter. In this case, the similar form of Eq. (13) and Eq. (16) suggests that we might only consider either static forces or dynamic forces in determining the departure diameter in practical use. The prediction of departure diameter by equating buoyancy and surface tension is

justified by the fact that there is a contact area between a growing bubble and the wall, and that the surface tension force decreases rapidly to zero only when the bubble begins to separate from the wall. Theoretically this method slightly underestimates the departure diameter. The equating of the buoyancy and dynamic forces is always true under the consideration that the separation happens only when the surface tension force tends to zero [3,13]. For a bubble growing on an enhanced surface, the separation is more dynamic-controlled. Therefore, the latter approach could give a more accurate prediction of the bubble departure diameter.

7 Concluding remarks

A detailed analysis has been performed for evaluating various forces acting on a bubble growing on horizontal heated tubular surfaces by using directly measured bubble geometric data and adopting appropriate correlations. The calculation results are demonstrated to be more reasonable than other methods used so far.

This work also reveals the forces acting on a bubble growing on an enhanced tube with re-entrant tunnels. It has been shown that the dynamic forces play a more important role in the bubble growth on an enhanced surface than on a smooth surface. A correlation for predicting the bubble departure diameter on an enhanced surface was derived from the force balance. This correlation has a similar form like the commonly used correlation for smooth tubes though it bares a different physical meaning.

In cases where both the static and dynamic forces are equally important, two approaches can be used to derive bubble departure equations: 1) equating buoyancy and surface tension forces, and, 2) equating buoyancy and dynamic forces.

Acknowledgements This work is partially funded by the Commission of the European Community. The financial support from Friedrich-Ebert-Stiftung for the doctoral study of one of the authors, Yuming Chen, and the support provided by Wieland-Werke AG, Ulm are greatly appreciated.

Received 13 September 2002

References

[1] Chen Y., Groll M., Mertz R. and Kulenovic R.: *Comparison of pool boiling bubble dynamics on smooth and enhanced tubes*, Int. J. Heat & Tech., **20**(2002), No.1, 3-14.

[2] Cole R.: *A photographic study of pool boiling in the region of the critical heat transfer*, AIChE J., **6**(1960), No. 4, 533-538.

[3] Roll J. B. and Myers J. E.: *The effect of surface tension on factors in boiling heat transfer*, AIChE J., **10**(1964), 530-534.

[4] Keshok E. G. and Siegel, R.: *Forces acting on bubbles in nucleate boiling under normal and reduced gravity conditions*, NASA Tech. Note TN D-2299, 1964.

[5] Cochran T. H., Aydelott J. C. and Frysinger T. C.: *The effect of subcooling and gravity level on boiling in the discrete bubble region*, NASA Tech. Note TN D-3449, 1966.

[6] Siegel R.: *Effects of reduced gravity on heat transfer*, Adv. in Heat Transfer, **4**(1967), 143-228.

[7] Rehm T. R.: *Bubble growth parameters in saturated and subcooled nucleate boiling*, Chem. Eng. Prog. Symp. Ser., **64**(1968), 88-94.

[8] Voloshko A. A. and Vurgaft A. V.: *Dynamics of vapor-bubble breakoff under free-convection boiling condition*, Heat Transfer – Soviet Research, **2**(1970), No. 6, 136-141.

[9] Hatton A. P., James D. D. and Liew T. L.: *Measurement of bubble characteristics for pool boiling from single cylindrical cavities*, Proc. 4^{th} Int. Heat Transfer Conf., Paris, France, Vol. V, B1.2, 1970.

[10] Kirichenko Y. A.: *Evaluation of the conditions of vapor bubble separation during nucleate boiling*, J. of Eng. Phys., **25**(1973), No. 1, 811-817.

[11] Saini J. S., Gupta C. P. and Lal S.: *Effect of Jakob number on forces controlling bubble departure in nucleate pool boiling*, Int. J. of Heat and Mass Transfer, **18**(1975), 472-474.

[12] Golorin V. S., Kol'Chugin B. A. and Zakharova E. A.: *Investigation of the mechanism of nucleate boiling of ethyl alcohol and benzene by means of high-speed motion-picture photography*, Heat Transfer – Soviet Research, **10**(1978), No. 4, 79-98.

[13] Zeng L. Z., Klausner J. F. and Mei R.: *A unified model for the prediction of bubble detachment diameters in boiling systems – I. Pool boiling*, Int. J. of Heat and Mass Transfer, **36**(1993), 2261-2270.

[14] Ginet N., Cioulachtjian S. and Lallemand M.: *Analysis of the forces acting on a single bubble of n-pentane growing on a horizontal wall*, Proc. 4^{th} Int. Conf. on *Multiphase Flow*, New Orleans, USA, Paper No. 840, 2001.

[15] Johnson M. A., Javier de la Pena, Jr. and Mesler R. B.: *Bubble shapes in nucleate boiling*, AIChE J., **12**(1966), No. 2, 344-348.

[16] Cornwell K. and Grant I. A.: *Heat transfer to bubbles under a horizontal tube*, Int. J. of Heat and Mass Transfer, **41**(1998), 1189-1197.

[17] Sakashita C. and Kumada T.: *Macrolayer formation and mechanisms of nucleate boiling, critical heat flux, and transition boiling*, Heat Transfer-Japanese Research, 27(2), 1998, 155-168.

[18] Milne-Thomson L. M.: *Theoretical Hydrodynamics*, 2nd Ed., The Macmillan Company, New York, 1950.

[19] Cole R. and Shulman H. L.: *Bubble departure diameters at subatmospheric pressures*, Chem. Eng. Prog. Symp. Ser., **62**(1966), 6-16.

[20] Peebles F. N. and Garbel H. J.: *Studies on the motion of gas bubbles in liquids*, Chem. Eng. Prog., **49**(1953), No. 2, 88-97.

[21] Kupferberg A. and Jameson G. J.: *Bubble formation at a submerged orifice above a gas chamber of finite volume*, Trans. Instn Chem. Engrs, **47**(1969), T241-T250.

[22] Khurana A. K. and Kumar R.: *Studies in bubble formation-III*, Chem. Engi. Sci., **24**(1969), 1711-1723.

[23] Memblelson H. D.: *The prediction of bubble terminal velocities from wave theory*, AIChE J., **13**(1967), No. 2, 250-253.

[24] Nakayama W., Daikoku T., Kuwahara H. and Nakajima T.: *Dynamic model of enhanced boiling heat transfer on porous surfaces. Part II: Analytical modeling*, J. of Heat Transfer, **102**(1980), 451-456.

[25] Chien, L-H and Webb, R. L.: *A nucleate boiling model for structured enhanced surfaces*, Int. J. of Heat and Mass Transfer, **41**(1998), No. 14, 2183-2195.

[26] Buyevich Yu. A. and Webbon B. W.: *Dynamics of vapour bubble in nucleate boiling*, Int. J. of Heat and Mass Transfer, **39**(1996), 2409-2426.

[27] Chen Y. and Groll M.: *Study on bubble dynamics by simulating the shape of bubble on heating surfaces*, Tech. Note, IKE-5TN-1733-02, 2002.